Linearly Distributed Antenna Diversity Using Single Frequency Network for High-Speed Railway Communications

Jimmy Hadi SUSANTO† Hiroyuki MIYAZAKI† Katsuhiro TEMMA† Tetsuya YAMAMOTO†
Tatsunori OBARA† and Fumiyuki ADACHI‡
Dept. of Communications Engineering, Graduate School of Engineering, Tohoku University
6-6-05 Aza-Aoba, Aramaki, Aoba-ku, Sendai, 980-8579 Japan
E-mail: †{jimmy, miyazaki, tenma, yamamoto, obara}@mobile.ecei.tohoku.ac.jp, ‡adachi@ecei.tohoku.ac.jp

***Abstract*—Broadband data services are demanded even under high mobility environment, such as high-speed railway. In this paper, we consider single-carrier (SC) linearly distributed antenna network (DAN). The distributed antenna-mobile terminal (MT) link will be a line-of-sight link and therefore, fading can be characterized as the frequency-selective Nakagami-Rice fading. Distributed antenna diversity using single frequency network (SFN) can mitigate the impacts of path and shadowing losses as well as the frequency-selective fading. In this paper, frequency-domain space-time block coded-joint transmit/receive diversity (FD-STBC-JTRD) is employed as SFN linearly distributed antenna diversity. It is confirmed by computer simulation that FD-STBC-JTRD is a powerful diversity to improve the transmission performance under a high mobility environment.**

Keywords—component; Distributed antennas, Nakagami-Rice fading, single frequency network, transmit/receive diversity

I. INTRODUCTION

In next generation mobile communication systems, high data-rate services are demanded even under high mobility environment, e.g. high-speed railway. However, large transmit power is necessary to provide high data-rate services. Since the available transmit power is limited especially in mobile terminal (MT), transmission power has to be reduced. Distributed antenna network (DAN) [1]-[4] is one promising solution to overcome this problem. A combination of DAN and antenna diversity can significantly reduce the transmission power [5]. For the case of high-speed railway communications, distributed antennas can be linearly placed along a railway line. The impacts of path and shadowing losses as well as the frequency-selective fading can be mitigated by using distributed antenna diversity using single frequency network (SFN). Since the antennas can be expected to be placed near the railway line, the channel can be characterized by Nakagami-Rice fading.

In this paper, we consider the frequency-domain space-time block coded-joint transmit/receive diversity (FD-STBC-JTRD) [6][7] downlink for single carrier (SC) SFN linearly distributed antenna diversity. FD-STBC-JTRD requires the channel state information (CSI) at the base station (BS) transmitter while requiring simple addition/subtraction and conjugate operation at receiver. Furthermore, it allows an arbitrary number of transmit antennas while keeping STBC coding rate the same. Therefore, FD-STBC-JTRD is suitable for the downlink (BS-to-MT) application to alleviate the complexity problem of MT receiver.

The rest of the paper is organized as follows. The fading model is presented in Section II. This is followed by description of SFN distributed antenna diversity in Section III. In Section IV, computer simulation results on the downlink throughput are discussed. Finally, conclusions and future works are drawn in Section V.

II. FREQUENCY-SELECTIVE NAKAGAMI-RICE FADING MODEL

A. DAN for High Speed Railway Communications

Figure 1 illustrates the system model considered in this paper. Distributed antennas are linearly located at distance R intervals on a straight line and connected by optical fiber to the signal processing center (SPC). The distributed antenna line and the railway line are separated by βR. It is assumed that the train is moving at a speed v. MT in a train car has N_r antennas. N_t distributed antennas closest to the MT are selected for antenna diversity.

B. Channel Model

In this paper, the frequency-selective Nakagami-Rice fading is considered. Figure 2 shows frequency-selective Nakagami-Rice fading channel model for linearly distributed antenna diversity using SFN. The channel is assumed to be composed of N_t direct paths, which is the same as the number of selected distributed antennas, and L discrete delay paths. Delay paths are scattered by circular scatter clusters around each distributed antenna and arrive to the MT from 360 degrees direction.

It is also assumed that the delay time of propagation paths is longer than those of direct paths as shown in Fig. 3, and the

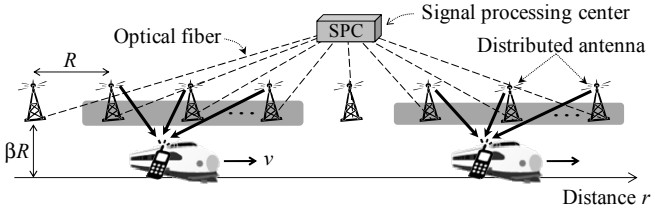

Fig. 1. DAN model.

978-1-4673-6050-0/13/$31.00 ©2013 IEEE

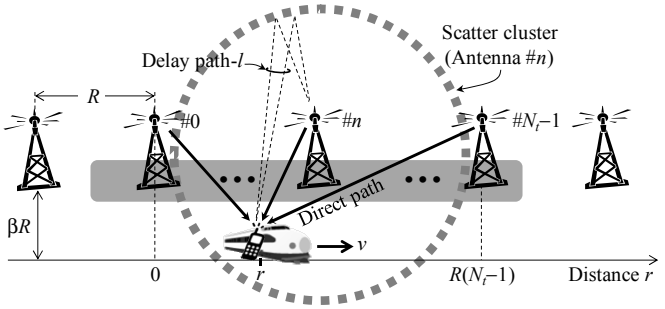

Fig. 2. Channel model.

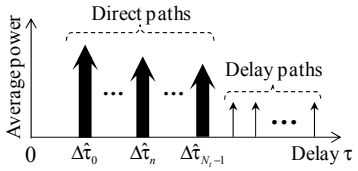

Fig. 3. Channel impulse response.

delay paths of each distributed antenna arrive at the MT at the same time. Rician K-factor of fading channel is assumed to be same for all channels between distributed antennas and MT.

The channel impulse response between the n-th distributed antenna and the m-th MT antenna $h_{m,n}(\tau)$ can be expressed as

$$h_{m,n}(\tau)=\sqrt{\frac{K}{K+1}}\hat{h}_{m,n}\delta(\tau-\hat{\tau}_{m,n})+\sqrt{\frac{1}{K+1}}\sum_{l=0}^{L-1}\tilde{h}_{m,n,l}\delta(\tau-\tilde{\tau}_{m,n,l}), \quad (1)$$

where K is Rician K-factor. $\hat{\tau}_{m,n}$ and $\tilde{\tau}_{m,n,l}$ denote delay time of direct path and l-th delay path between n-th distributed antenna and m-th MT antenna, respectively. $\hat{h}_{m,n}$ and $\tilde{h}_{m,n,l}$ are respectively complex-valued channel gains, including the impact of the path loss, of direct path and l-th delay path between n-th distributed antenna and m-th MT antenna. They are given as

$$\hat{h}_{m,n}=\sqrt{u_n^{-\alpha}}\hat{h}'_{m,n}, \quad (2\text{-a})$$

$$\tilde{h}_{m,n,l}=\sqrt{u_n^{-\alpha}}\tilde{h}'_{m,n,l}, \quad (2\text{-b})$$

where u_n is distance between n-th distributed antenna and MT and α is path loss exponent. $\hat{h}'_{m,n}$ and $\tilde{h}'_{m,n,l}$ are respectively complex-valued channel gains of direct path and l-th delay path between n-th distributed antenna and m-th MT antenna that fluctuate due to fading.

The instantaneous received signal power $P_{r,n}$ at the MT from n-th distributed antenna can be expressed as

$$P_{r,n}=p_{t,n}\cdot u_n^{-\alpha}\cdot\sum_{m=0}^{N_r-1}\left\{\frac{K}{K+1}\left|\hat{h}'_{m,n}\right|^2+\frac{1}{K+1}\sum_{l=0}^{L-1}\left|\tilde{h}'_{m,n,l}\right|^2\right\}, \quad (3)$$

where $p_{t,n}$ is the transmit power from the n-th distributed antenna. The total transmit power from one distributed antenna is kept constant as p_t. Eq. (3) can be rewritten as

$$\begin{aligned}P_{r,n}&=\left(p_{t,n}\cdot R^{-\alpha}\right)\cdot\left(u_n/R\right)^{-\alpha}\cdot\\&\quad\sum_{m=0}^{N_r-1}\left\{\frac{K}{K+1}\left|\hat{h}'_{m,n}\right|^2+\frac{1}{K+1}\sum_{l=0}^{L-1}\left|\tilde{h}'_{m,n,l}\right|^2\right\} \quad (4)\\&=P_{t,n}\cdot U_n^{-\alpha}\cdot\sum_{m=0}^{N_r-1}\left\{\frac{K}{K+1}\left|\hat{h}'_{m,n}\right|^2+\frac{1}{K+1}\sum_{l=0}^{L-1}\left|\tilde{h}'_{m,n,l}\right|^2\right\}\end{aligned}$$

where $P_{t,n}$ is the normalized transmit power and U_n is the normalized distance between n-th distributed antenna and the MT. They are given as

$$P_{t,n}=p_{t,n}\cdot R^{-\alpha}, \quad (5)$$

$$U_n=u_n/R. \quad (6)$$

III. SFN Distributed Antenna Diversity

In this paper, we employ FD-STBC-JTRD as the SFN linearly distributed antenna diversity. For comparison, we also evaluate the performance of simultaneous transmission which is a simple diversity scheme.

A. FD-STBC-JTRD

Figure 4 illustrates the transmitter/receiver structure of downlink FD-STBC-JTRD. At the SPC, a sequence of $J\times N_c$ data modulated symbols to be transmitted is divided into a sequence of J blocks of N_c symbols each. N_c-point fast fourier transform (FFT) is applied to convert the j-th symbol block $\{d_j(t);\ t=0\sim N_c-1\}$, $j=0\sim J-1$, into the frequency-domain signal $\{D_j(k);\ k=0\sim N_c-1\}$, $j=0\sim J-1$, as

$$D_j(k)=\sum_{t=0}^{N_c-1}d_j(t)\exp\left(-j2\pi k\frac{t}{N_c}\right). \quad (7)$$

A sequence of J frequency-domain signals, $\{D_j(k);\ k=0\sim N_c-1\}$, is encoded into $N_r\times Q$ coded frequency-domain signal block $\mathbf{\Omega}_{N_r}(k)$ each. The data symbol block length J and the coding-sequence length Q of FD-STBC-JTRD depend on the number N_r of receive antennas. The relationship of N_r, J, Q and coding rate $R_{\text{STBC-JTRD}}$ (=J/Q) is shown in table I.

STBC encoding matrix $\mathbf{\Omega}_{N_r}(k)$ $N_r\times Q$ is given as

$$\mathbf{\Omega}_{N_r=1}(k)=D_0(k), \quad (8\text{-a})$$

$$\mathbf{\Omega}_{N_r=2}(k)=\begin{pmatrix}D_0(k) & -D_1^*(k)\\ D_1(k) & D_0^*(k)\end{pmatrix}, \quad (8\text{-b})$$

$$\mathbf{\Omega}_{N_r=3}(k)=\begin{pmatrix}D_0(k) & -D_1^*(k) & -D_2^*(k) & 0\\ D_1(k) & D_0^*(k) & 0 & -D_2^*(k)\\ D_2(k) & 0 & D_0^*(k) & D_1^*(k)\end{pmatrix}, \quad (8\text{-c})$$

$$\mathbf{\Omega}_{N_r=4}(k)=\begin{pmatrix}D_0(k) & -D_1^*(k) & -D_2^*(k) & 0\\ D_1(k) & D_0^*(k) & 0 & -D_2^*(k)\\ D_2(k) & 0 & D_0^*(k) & D_1^*(k)\\ 0 & D_2(k) & -D_1(k) & D_0(k)\end{pmatrix}. \quad (8\text{-d})$$

After STBC encoding, the transmit frequency-domain equalization (FDE) is applied. N_t streams of Q coded frequency-domain signal block $\mathbf{X}(k)$ of size $N_t\times Q$ after the transmit FDE can be expressed using the matrix form as

$$\mathbf{X}(k)=\sqrt{2E_s/T_s}C\mathbf{W}^H(k)\mathbf{\Omega}_{N_r}(k), \quad (9)$$

where E_s and T_s denote transmit symbol energy and symbol duration, respectively, and C is the power normalization factor, to keep the average transmit power constant, given as

$$C=\sqrt{\frac{N_c}{\sum_{n=0}^{N_t-1}\sum_{m=0}^{N_r-1}\sum_{k=0}^{N_c-1}\left|W_{n,m}(k)\right|^2}}, \quad (10)$$

TABLE I. RELATIONSHIP OF STBC-JTRD

N_t	N_r	J	Q	$R_{\text{STBC-JTRD}}$
Arbitrary	1	1	1	1
	2	2	2	1
	3	3	4	3/4
	4	3	4	3/4

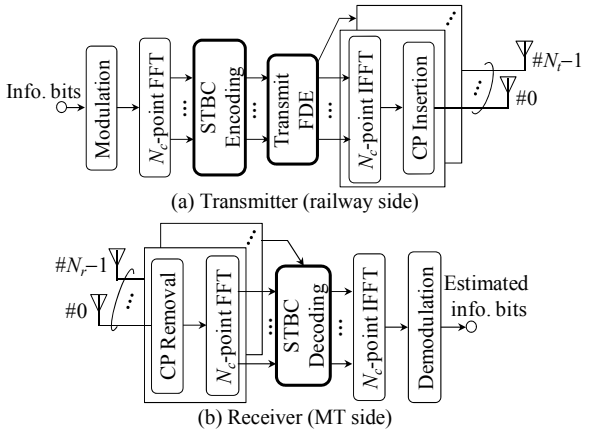

Fig. 4. Structure of FD-STBC-JTRD.

where $W_{n,m}(k)$ is the element of transmit FDE matrix $\mathbf{W}(k)$. In this paper, we use the following transmit FDE weight [8]

$$W_{m,n}(k)=\frac{H_{m,n}(k)}{\frac{1}{N_r}\sum_{n=0}^{N_t-1}\sum_{m=0}^{N_r-1}\left|H_{m,n}(k)\right|^2+\left(E_s/N_0\right)^{-1}}, \tag{11}$$

where N_0 is the single-sided power spectrum density of additive white Gaussian noise (AWGN) and $H_{m,n}(k)$ denotes the frequency-domain channel transfer function of the link between n-th distributed antenna and m-th MT antenna given as

$$\begin{aligned}H_{m,n}(k)=&\sqrt{\frac{K}{K+1}}\hat{h}_{m,n}\exp\left(-j2\pi k\frac{\hat{\tau}_{m,n}}{N_c}\right)\\&+\sqrt{\frac{1}{K+1}}\sum_{l=0}^{L-1}\tilde{h}_{m,n,l}\exp\left(-j2\pi k\frac{\tilde{\tau}_{m,n,l}}{N_c}\right)\end{aligned}. \tag{12}$$

Finally, N_c-point inverse FFT (IFFT) is applied to $\mathbf{X}(k)$ to obtain the time-domain codeword. After inserting the cyclic prefix (CP) of N_g symbols into the guard interval (GI), N_t streams of (N_c+N_g) symbol blocks each are transmitted from N_t distributed antennas.

B. FD-STBC-JTRD Decoding

At the MT, after CP removal, N_r received signals are transformed by N_c-point FFT into the frequency-domain signals. The (m,q)th element $Y_{m,q}(k)$ of the frequency-domain received signal matrix $\mathbf{Y}(k)$ can be expressed as

$$Y_{m,q}(k)=\sum_{n=0}^{N_t-1}H_{m,n}(k)X_{n,q}(k)+\Pi_{m,q}(k), \tag{13}$$

where, $X_{n,q}(k)$ is the q-th frequency-domain symbol block transmitted from the n-th distributed antenna and $\Pi_{m,q}(k)$ is i.i.d. complex Gaussian variable having zero mean and variance $2N_0/T_s$.

Then, in each frequency component, FD-STBC-JTRD decoding is carried out. STBC decoded received symbol vector $\hat{\mathbf{D}}_{N_r}(k)$ is given as

$$\hat{\mathbf{D}}_{N_r=1}(k)=\hat{D}_0(k)=Y_{0,0}(k), \tag{14-a}$$

$$\hat{\mathbf{D}}_{N_r=2}(k)=\begin{pmatrix}\hat{D}_0(k)\\ \hat{D}_1(k)\end{pmatrix}=\begin{pmatrix}Y_{0,0}(k)+Y_{1,1}^*(k)\\ Y_{1,0}(k)-Y_{0,1}^*(k)\end{pmatrix}, \tag{14-b}$$

$$\hat{\mathbf{D}}_{N_r=3}(k)=\begin{pmatrix}\hat{D}_0(k)\\ \hat{D}_1(k)\\ \hat{D}_2(k)\end{pmatrix}=\begin{pmatrix}Y_{0,0}(k)+Y_{1,1}^*(k)+Y_{2,2}^*(k)\\ Y_{1,0}(k)-Y_{0,1}^*(k)+Y_{2,3}^*(k)\\ Y_{2,0}(k)-Y_{0,2}^*(k)-Y_{1,3}^*(k)\end{pmatrix}, \tag{14-c}$$

$$\hat{\mathbf{D}}_{N_r=4}(k)=\begin{pmatrix}\hat{D}_0(k)\\ \hat{D}_1(k)\\ \hat{D}_2(k)\end{pmatrix}=\begin{pmatrix}Y_{0,0}(k)+Y_{1,1}^*(k)+Y_{2,2}^*(k)+Y_{3,3}(k)\\ Y_{1,0}(k)-Y_{0,1}^*(k)+Y_{2,3}^*(k)-Y_{3,2}(k)\\ Y_{2,0}(k)-Y_{0,2}^*(k)-Y_{1,3}^*(k)+Y_{3,1}(k)\end{pmatrix}. \tag{14-d}$$

Finally, N_c-point IFFT is applied to obtain time-domain soft decision symbol. As understood from Eqs. (14-a)-(14-d), FD-STBC-JTRD decoding needs only addition/subtraction and conjugate operations, and hence it can keep MT receiver's complexity low.

C. Simultaneous Transmission

Figure 5 shows the transmitter and receiver structure of downlink simultaneous transmission in distributed antenna diversity using SFN. At the transmitter, after CP insertion, the transmit symbol blocks $\{\xi(t): t=0\sim N_c-1\}$ are transmitted from N_t distributed antennas.

At the MT, after removing CP from received signal block, the time-domain received signal is transformed into the frequency-domain received signal by N_c-point FFT. The frequency-domain received signal vector $\mathbf{\Psi}(k)=\left[\Psi_0(k),\cdots,\Psi_{N_r-1}(k)\right]^T$ can be expressed as

$$\begin{aligned}\mathbf{\Psi}(k)&=\sqrt{2E_s/T_s}\begin{bmatrix}\sum_{n=0}^{N_t-1}H_{0,n}(k)\\ \vdots\\ \sum_{n=0}^{N_t-1}H_{N_r-1,n}(k)\end{bmatrix}\Xi(k)+\begin{bmatrix}\Pi_0(k)\\ \vdots\\ \Pi_{N_r-1}(k)\end{bmatrix}\\&=\sqrt{2E_s/T_s}\begin{bmatrix}\overline{H}_0(k)\\ \vdots\\ \overline{H}_{N_r-1}(k)\end{bmatrix}\Xi(k)+\mathbf{\Pi}(k)\\&=\sqrt{2E_s/T_s}\,\overline{\mathbf{H}}(k)\Xi(k)+\mathbf{\Pi}(k)\end{aligned}, \tag{15}$$

where $\Xi(k)$ is k-th frequency component of the transmitted signal and $\Pi_m(k)$ is i.i.d. complex-valued AWGN at m-th MT antenna having zero mean and variance $2N_0/T_s$.

The receive FDE and diversity combining are jointly carried out as follows.

$$\hat{\Psi}(k)=\mathbf{W}^T(k)\mathbf{\Psi}(k)=\sum_{m=0}^{N_r-1}W_m(k)\cdot\Psi_m(k), \tag{16}$$

where $\mathbf{W}^T(k)=\left[W_0(k),\cdots,W_{N_r-1}(k)\right]$ is the weight matrix and is determined so as to minimize the mean square error (MSE)

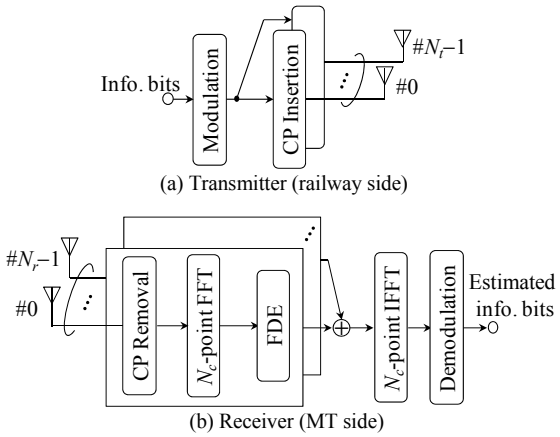

Fig. 5. Structure of simultaneous transmission.

between the transmitted signal $\Xi(k)$ and the signal $\hat{\Psi}(k)$ after joint FDE and diversity combining [9] given as

$$W_m(k) = \frac{\overline{H}_m^*(k)}{\sum_{m=0}^{N_r-1}\left|\overline{H}_m(k)\right|^2 + \left(E_s/N_0\right)^{-1}}. \quad (17)$$

The frequency-domain signal after joint FDE/diversity combining is transformed back to the time-domain signal by N_c-point IFFT for data demodulation.

IV. Simulation Results

We evaluate the downlink throughput performance of linearly distributed antenna diversity using SFN under Nakagami-Rice fading environment. The parameters are summarized in Table II. The distance between distributed antennas R and the distance between distributed antenna line and railway line βR are assumed to be 1(km) and 10(m), respectively. We consider QPSK data modulation. FFT block size N_c=512 symbols, and GI length N_g=112 symbols, respectively. The channel is assumed to be frequency-selective

TABLE II. Simulation Parameters

Transmitter	Modulation	QPSK
	Block size N_c	512
	CP length N_g	112
	Packet size	1024(bits)
	Distributed antenna spacing R	1(km)
	Distributed antenna-railway spacing βR	10(m)
	FDE weight	MMSE
	Channel estimation	Ideal
	Normalized transmit E_s/N_0/ant.	−1.5dB
Channel	K-Factor	3, 5, 10
	No. of delay paths	16
	Path loss exponent	3.5
	Symbol length T_s	0.1(μs)
	Carrier frequency	2(GHz)
Receiver	No. of MT antenna	2
	MT antenna spacing	0.5λ

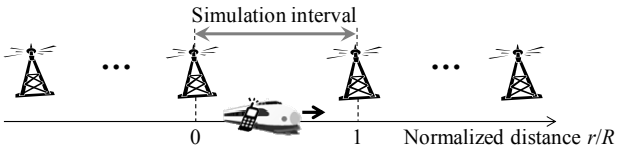

Fig. 6. Simulation model.

Nakagami-Rice fading channel which is composed of N_t direct paths and L=16 discrete delay paths. Ideal channel estimation at the railway side is assumed. The number of MT antenna is set to N_r=2 and antenna separation is set to a half of carrier wavelength λ.

Signal is transmitted from N_t distributed antennas, which have constant normalized transmit E_s/N_0 per distributed antenna, to N_r=2 MT antennas while moving MT from point 0 to 1 as shown in Fig. 6. This procedure is repeated sufficient number of times to measure the throughput (bps/Hz) distribution. Throughput is calculated by

$$Throughput = \frac{\log_2 M \times N_c}{(N_c + N_g)} \cdot (1 - PER) \cdot R_{STBC-JTRD}, \quad (18)$$

where M is number of modulation level and PER is packet error rate.

Figure 7 shows the throughput distribution obtained by using FD-STBC-JTRD and simultaneous transmission. The rician K-factor is set as K=5, and normalized transmit E_s/N_0 per distributed antenna is set to −1.5dB. From Fig. 7, it can be seen that the average throughput degrades at the center point (r/R=0.5) due to the path loss. It is also seen from Fig. 7 that there are regions that throughput performance of FD-STBC-JTRD is smaller than simultaneous transmission. This is because the noise enhancement occurs by the addition/subtraction of the received signal in STBC decoding. However, at the center point FD-STBC-JTRD can achieve 1.3 times higher throughput than simultaneous transmission. This is because FD-STBC-JTRD can obtain higher spatial diversity gain than the simultaneous transmission.

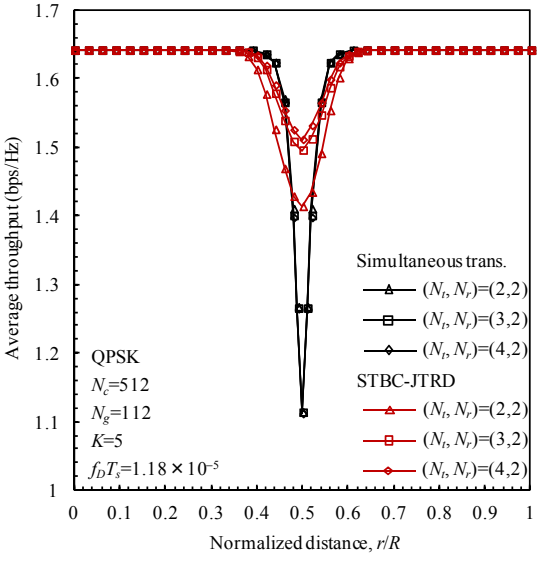

Fig. 7. Throughput distribution obtained by FD-STBC-JTRD and simultaneous transmission.

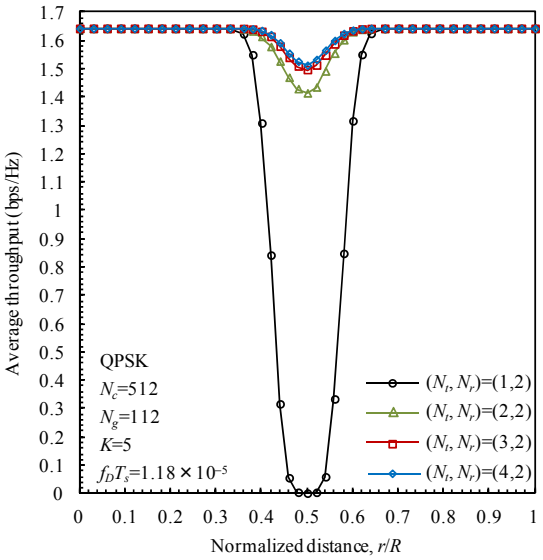

Fig. 8. Throughput distribution obtained by FD-STBC-JTRD.

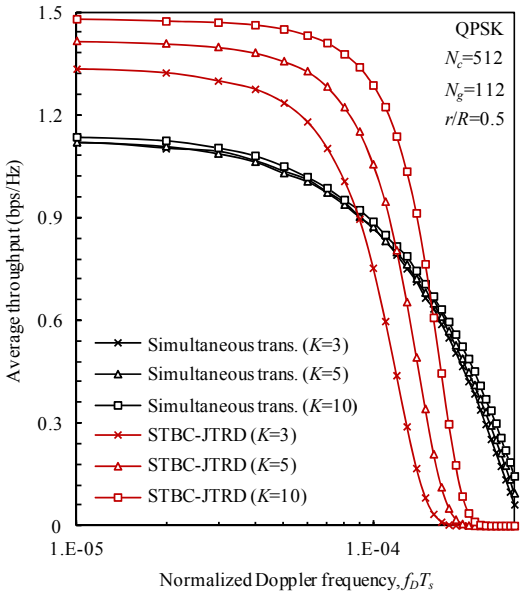

Fig. 9. Impact of normalized Doppler frequency.

Figure 8 plots the throughput distribution obtained by FD-STBC-JTRD with the number of distributed antenna as parameter. It can be seen from Fig.8 that the throughput performance of FD-STBC-JTRD improves as the number N_t of distributed antennas used in SFN increases. However, the throughput only slightly improves when N_t becomes more than 3. This is because the propagation path loss of the link between MT and the third or more distributed antenna is high, and hence, their contribution gets smaller.

Figure 9 shows the impact of normalized Doppler frequency f_DT_s in throughput performance at the center point. Assuming 10MHz signal bandwidth at the carrier frequency 2GHz, the normalized Doppler frequency $f_DT_s=10^{-4}$ corresponds to a travelling speed of 540km/h. It is shown from the result that the average throughput performance improves as K-factor increases, both in simultaneous transmission and FD-STBC-JTRD, because the time fluctuation of fading becomes smaller as K-factor increases. It is also seen from Fig. 9 that although the FD-STBC-JTRD throughput degrades as the fading rate gets higher due to the interference between STBC code words, it is still better than the simultaneous transmission in low f_DT_s region (1.3 times for K=5 and 1.2 times for K=3 at $f_DT_s=5\times10^{-5}$).

V. Conclusion

In this paper, we evaluated, by computer simulation, the downlink throughput achievable using SFN linearly distributed antenna diversity under a high mobility environment. As downlink diversity, FD-STBC-JTRD and simultaneous transmission were considered. We showed that the use of two distributed antennas is sufficient to improve the FD-STBC-JTRD performance and that although the FD-STBC-JTRD degrades as the fading rate gets higher due to the interference between STBC code words, it is still better than the simultaneous transmission as far as the normalized Doppler frequency $f_DT_s<10^{-4}$.

In this paper, ideal channel estimation was assumed. Channel estimation in a very high mobility environment is practically important future work. To improve the FD-STBC-JTRD performance in a very high mobility environment is also an interesting future work.

References

[1] A. A. M. Saleh, A. J. Rustako, and R. S. Roman, "Distributed antennas for indoor radio communications," IEEE Trans. Commun., vol.35, no.12, pp.1245-1251, Dec. 1987.

[2] W. Choi, and J. G. Andrews, "Downlink performance and capacity of distributed antenna systems in a multicell environment," IEEE Trans. Wireless Commun., vol.6, no.1, Jan. 2007.

[3] E. Kudoh and F. Adachi, "Study of a multi-hop communication in a virtual cellular system," Proc. 6th International Symposium on Wireless Personal Multimedia Communications, vol.3, pp.261-265, 19-22 Oct. 2003.

[4] H. Matsuda, H. Tomeba, and F. Adachi, "Channel capacity of distributed antenna system using maximal ratio transmission," Proc. The 5th IEEE VTS Asia Pacific Wireless Communications Symposium, 21-22 Aug. 2008.

[5] R. Matsukawa, T. Obara, K. Takeda, and F. Adachi, "Downlink throughput performance of distributed antenna network using transmit/receive diversity," Proc. The 74th IEEE Vehicular Technology Conference, 5-8 Sep. 2011.

[6] H. Tomeba, K. Takeda, and F. Adachi, "Space-time block coded-joint transmit/receive diversity in a frequency-nonselective rayleigh fading channel," IEICE Trans. Commun., vol.E89-B, no.8, pp.2189-2195, Aug. 2006.

[7] H. Tomeba, K. Takeda, and F. Adachi, "Space-time block coded-joint transmit/receive diversity using more than 4 receive antennas," Proc. The 68th IEEE Vehicular Technology Conference, 21-25 Sep. 2008.

[8] H. Tomeba, K. Takeda, and F. Adachi, "Frequency-domain space-time block coded-joint transmit/receive diversity for the single carrier transmission," Proc. The 10th IEEE International Conference on Communication Systems, 30 Oct.-1 Nov. 2006.

[9] F. Adachi and T. Sao, "Joint antenna diversity and frequency-domain equalization for multi-rate MC-CDMA," IEICE Trans. Commun., vol.E86-B, no.11, pp.3217-3224, Nov. 2003.